In Silico Evolved *lac* Operons Exhibit Bistability for Artificial Inducers, but Not for Lactose

M. J. A. van Hoek and P. Hogeweg
Theoretical Biology/Bioinformatics Group, Utrecht University, Utrecht, The Netherlands

ABSTRACT Bistability in the *lac* operon of *Escherichia coli* has been widely studied, both experimentally and theoretically. Experimentally, bistability has been observed when *E. coli* is induced by an artificial, nonmetabolizable, inducer. However, if the *lac* operon is induced with lactose, the natural inducer, bistability has not been demonstrated. We derive an analytical expression that can predict the occurrence of bistability both for artificial inducers and lactose. We find very different conditions for bistability in the two cases. Indeed, for artificial inducers bistability is predicted, but for lactose the condition for bistability is much more difficult to satisfy. Moreover, we demonstrate that in silico evolution of the *lac* operon generates an operon that avoids bistability with respect to lactose, but does exhibit bistability with respect to artificial inducers. The activity of this evolved operon strikingly resembles the experimentally observed activity of the operon. Thus our computational experiments suggest that the wild-type *lac* operon, which regulates lactose metabolism, is not a bistable switch. Nevertheless, for engineering purposes, this operon can be used as a bistable switch with artificial inducers.

INTRODUCTION

Since the discovery of the *lac* operon of *Escherichia coli* (1), it has been a model study for genetic regulation. The *lac* operon simultaneously regulates the transcription of three genes, LacZ, LacY, and LacA. Only LacZ and LacY are important for lactose utilization. LacZ codes for β-galactosidase, the protein responsible for lactose degradation and lacY codes for a membrane permease protein, which transports the lactose into the cell.

The expression of the *lac* operon depends on the internal concentration of two molecules, allolactose and cAMP. Allolactose is derived from lactose, while glucose influx into the cell represses cAMP. Both allolactose and cAMP induce the operon and therefore, classically, the *lac* operon is described as a Boolean function: lactose and not glucose.

Both the permease and β-galactosidase are needed to produce allolactose, and allolactose again induces the operon. Therefore, there is an inherent positive feedback loop in the system that can cause bistability (2). This bistability is caused by a fold bifurcation.

This bistable behavior has already been observed by Novick and Weiner (3). It was observed that a genetically identical population of *E. coli* can be heterogeneous in its activity of the operon, while the environment is the same for the whole population. These experiments were performed using an artificial inducer of the operon. These inducers, such as isopropyl β-*D*-thiogalactopyranoside (IPTG) and thiomethyl β-D-galactoside (TMG), cannot be metabolized by β-galactosidase, in contrast to lactose, the natural inducer.

Recent advances in experimental techniques that allow direct measurement of the promoter activity have shed new light on the *lac* operon. The activity of the operon in living cells has been measured (4). It was found that the operon is an intricate function of the cAMP and inducer concentration, with four different threshold values and plateau transcription levels. Furthermore, shallow switches were observed, which need approximately a 10-fold change in cAMP or inducer concentration, all in contrast to the classical AND-gate. Furthermore, bistability of the *lac* operon on the single cell level has been observed (5). This study confirmed previous findings that the operon behaves bistably with respect to artificial inducers. However, interestingly, bistability could not be demonstrated when growing on lactose, the natural inducer of the operon. Finally, it has been shown that *E. coli* can optimize its operon activity in only a few hundred generations (6).

Several theoretical models, using detailed parameter values, have been developed that explain the occurrence of bistability in the *lac* operon, both for induction by artificial inducers (7) and by lactose (8). These detailed theoretical models have two important drawbacks. First, the outcome depends highly on the parameter values used. Notwithstanding extensive experimental work, these parameter values are still not very reliable. Second, these detailed models are not analytically solved, and therefore it is difficult to know which parts of the model contribute to the bistability. Therefore, the modeling is still far from conclusive.

Here we try to avoid these shortcomings in two ways. First, by making an approximation of our model we are able to find an analytical expression that predicts under which conditions operons are bistable, both for artificial inducers and lactose. Second, by in silico evolution of the *lac* operon in a fluctuating environment of glucose and lactose, we let cells adapt their operons to the assumed biochemical parameters and their environment. In this way we can study under which environmental circumstances bistability will evolve.

Submitted November 8, 2005, and accepted for publication July 11, 2006.

Address reprint requests to M. J. A. van Hoek, Tel.: 31-30-2531497; E-mail: m.j.a.vanhoek@bio.uu.nl.

0006-3495/06/10/2833/11 $2.00

doi: 10.1529/biophysj.105.077420

The analytical expression we find indeed predicts bistability to occur for artificial inducers, whereas it also predicts that for lactose it is much more difficult to have a bistable switch. In our evolutionary simulations we find that, when starting with a bistable population, evolution drives the population out of the bistable region. When growing on artificial inducers, however, these evolved operons do behave bistably. Furthermore, the phase diagram of the in silico evolved *lac* operon is quantitatively very similar to the experimentally observed phase diagram (5).

We performed evolutionary simulations in different environments. Sometimes bistability at very high glucose concentrations was observed, but for lower glucose concentrations bistability was always avoided.

Our findings put the occurrence of bistability in the *lac* operon in a different perspective. Relative to lactose, bistability is avoided, and bistability relative to artificial inducers is a side-effect of evolution on lactose, the natural inducer of the *lac* operon.

METHODS

The dynamics of the *lac* operon

We developed a differential equation model, based on the model of Wong et al. (9), to describe the dynamics of the *lac* operon. The model consists of 10 differential equations describing glucose and lactose metabolism and regulation. Here we shortly describe the model equations. In the Supplementary Material the rationale of the model is explained in more detail.

Five of these 10 differential equations are important for the bistability in this system, namely the equations describing mRNA, M; β-galactosidase, B; permease, P; internal lactose, L; and allolactose, A. mRNA production is modeled after Setty et al. (4), while the other four equations are modeled after Wong et al. (9).

$$PA(A,C) \equiv V_1 \frac{1 + \frac{V_2 (C/k_C)^n}{1+(C/k_C)^n} + \frac{V_3}{1+(A/k_A)^m}}{1 + \frac{V_4 (C/k_C)^n}{1+(C/k_C)^n} + \frac{V_5}{1+(A/k_A)^m}}. \quad (1)$$

$$\frac{dM}{dt} = min(PA(A,C), V_{mRNA,max}) - (\gamma_M + \mu)M. \quad (2)$$

$$\frac{dB}{dt} = k_B M - (\gamma_B + \mu)B. \quad (3)$$

$$\frac{dP}{dt} = k_P M - (\gamma_P + \mu)P. \quad (4)$$

$$\frac{dL}{dt} = P\left(\frac{k_{Lac,in} L_{ext}}{K_{Lac,in} + L_{ext}} - \frac{k_{Lac,out} L}{K_{Lac,out} + L}\right) - B\frac{(k_{cat,Lac} + k_{Lac-Allo})L}{L + K_{m,Lac}} - (\gamma_L + \mu)L. \quad (5)$$

$$\frac{dA}{dt} = B\frac{k_{Lac-Allo} L}{L + K_{m,Lac}} - B\frac{k_{cat,Allo} A}{A + K_{m,Allo}} - (\gamma_A + \mu)A. \quad (6)$$

$PA(A, C)$ is defined as the promoter activity as a function of allolactose (A) and cAMP (C) and is a two-dimensional Hill-function, with coefficients m and n. cAMP is dependent on glucose uptake, while allolactose is dependent on lactose uptake. Glucose uptake is determined by the phosphoenolpyruvate: carbohydrate phosphotransferase system (PTS) (10). This system transports and phosphorylates external glucose, and cAMP production is repressed by this process; therefore, the internal glucose concentration is inversely related to the cAMP concentration.

Equation 2 describes transcription and degradation of mRNA. We impose a maximal transcription rate, similar to the maximal in vivo transcription rate (11) (see Supplementary Material), to avoid unrealistically high transcription rates during the evolutionary simulations.

The value μ is defined as the growth rate of the cell. We assume first-order degradation for all chemicals. Equations 3 and 4 describe translation of mRNA to β-galactosidase and permease. Equation 5 describes reversible lactose influx by permease, where L_{ext} is the external lactose concentration, and the degradation of internal lactose by β-galactosidase.

Inducer exclusion is not taken into account in our model for two reasons. First, lactose efflux does not depend on the external glucose concentration (9), because inducer exclusion only affects lactose influx. We will later show that only lactose efflux determines bistability in the *lac* operon. Secondly, although bistability is not affected by inducer exclusion, it does have an effect on the evolution of the promoter function. When inducer exclusion would be taken into account, cells would never experience high internal glucose and lactose concentrations simultaneously. Therefore, there would be no evolutionary pressure on this part of the promoter function. Because we did not want to impose any form of regulation, we did not take inducer exclusion into account.

Equation 6 describes production and degradation of allolactose by β-galactosidase. Note that, in contrast to Wong et al. (9), we added an operon-independent degradation rate of lactose and allolactose. Without these terms, bistability would only depend on the growth rate. When the growth rate then would be zero, bistability would not be possible, because the lactose and allolactose steady states would be independent of B and P.

Apart from these five differential equations that determine bistability, five more differential equations are needed to describe glucose uptake, metabolism, and growth. β-galactosidase degrades lactose to glucose and galactose. Internal glucose can be phosphorylated or, if the internal glucose concentration is very high (12), excreted to the medium. This gives for the internal glucose concentration

$$\frac{dG}{dt} = \frac{k_{cat,Lac} BL}{L + K_{m,Lac}} + \frac{k_{cat,Allo} BA}{A + K_{m,Allo}} - \frac{k_{cat,Glu} G}{G + K_{m,Glu}} - k_{Glu,out}(G - G_{ext}) - \mu G. \quad (7)$$

Besides internal glucose, glucose-6-phosphate is modeled separately. External glucose is transported inside the cell and phosphorylated by the PTS. Galactose formed by lactose degradation is also converted to glucose-6-phosphate. The glucose formed by lactose degradation is phosphorylated, as modeled in Eq. 7. Finally, glucose-6-phosphate is degraded by respiration and fermentation, such that glucose-6-phosphate is first respired and if the respiratory pathways are saturated, overflow is fermented (13):

$$\frac{dG6P}{dt} = \frac{k_{t,Glu} G_{ext}}{G_{ext} + K_{t,Glu}} + \frac{k_{cat,Lac} BL}{L + K_{m,Lac}} + \frac{k_{cat,Allo} BA}{A + K_{m,Allo}} + \frac{k_{cat,Glu} G}{G + K_{m,Glu}} - \frac{k_{G6P,Rsp} G6P}{G6P + K_{G6P,Rsp}} - \frac{k_{G6P,Frm} G6P^8}{K_{G6P,Frm}^8 + G6P^8} - \mu G6P. \quad (8)$$

Transcription of the *lac* operon depends on the cAMP concentration, which again depends inversely on glucose transport by the PTS. This is modeled as

$$\frac{dC}{dt} = k_{syn,cAMP} \frac{K_{syn,cAMP}}{\frac{k_{t,Glu} G_{ext}}{G_{ext} + K_{t,Glu}} + K_{syn,cAMP}} - (\gamma_{cAMP} + \mu)C. \quad (9)$$

Furthermore, we need a measure for the amount of energy the cells consume and produce, which determines their growth rate; this is done via ATP.

Energy-producing actions are respiration and fermentation. Energy-consuming actions are basal metabolism, growth, cost for *lac* operon activity, and a cost to convert galactose to glucose, which then gives

$$\frac{dATP}{dt} = \frac{Y_{\mathrm{Rsp}} k_{\mathrm{G6P,Rsp}} G6P}{G6P + K_{\mathrm{G6P,Rsp}}} + \frac{2k_{\mathrm{G6P,Frm}} G6P^8}{K_{\mathrm{G6P,Frm}}^8 + G6P^8} - BMC - GC\times\mu - PC \times PA(A,C) - \frac{k_{\mathrm{cat,Lac}} BL}{L + K_{\mathrm{m,Lac}}} - \frac{k_{\mathrm{cat,Allo}} BA}{A + K_{\mathrm{m,Allo}}}. \quad (10)$$

To determine the growth rate of the bacteria, we assume a relationship between the amount of ATP and the growth rate. We assume a sigmoid relationship between energy and growth, such that cell growth becomes

$$\frac{dX}{dt} = \mu_{\max} \frac{ATP^4}{ATP^4 + K_{\mathrm{ATP}}^4} X. \quad (11)$$

The evolutionary model

To study the evolution of the *lac* operon we developed an individual-oriented spatial model. A detailed description of this model can be found in the Supplementary Material.

The intracellular dynamics are determined by all 10 differential equations described in the previous section. A population of cells evolves the parameters that determine their promoter activity. These are the parameters of Eq. 1. The five different V-parameters consist of seven biological binding parameters (see Supplementary Material). These seven plus k_A, k_C, n, and m are being evolved, while all other parameters are kept constant.

Space has been shown to be crucial for the evolution of metabolic regulation (14). Without space, bacteria would never evolve to an efficient use of metabolites, but rather always consume the amount of metabolites that optimizes their growth rate at that time. Therefore, we choose to develop a spatially explicit model.

We model a population of a few hundred cells, on a square grid of 25 × 25 grid points, growing on a fluctuating environment of glucose and lactose. Because of the small population size, these cells should be interpreted as a colony of identical cells. In Fig. 1, a screen-shot of the model is shown.

These cells consume glucose and lactose according to the model described in the previous section. The cells divide (with possible mutation) if they have grown twice their original size, ''die'' in a density-dependent way (or when their energy, as described in Eq. 10 drops below zero), and perform a random walk across the grid.

Because we want the cells to adapt to a fluctuating environment, glucose and lactose influx are modeled in periods with and without glucose and lactose influx, which are independent of each other. The lengths of these periods are determined stochastically, but all have on average an equal length. The duration of the periods with and without glucose or lactose are chosen such that the cells can just adapt their protein levels to the new environment. However, we checked the results for longer and shorter periods. The glucose and lactose influx is homogeneously over the grid. Due to metabolism by the cells, the glucose and lactose concentration become heterogeneous (see Fig. 1). Glucose and lactose diffuse over the grid.

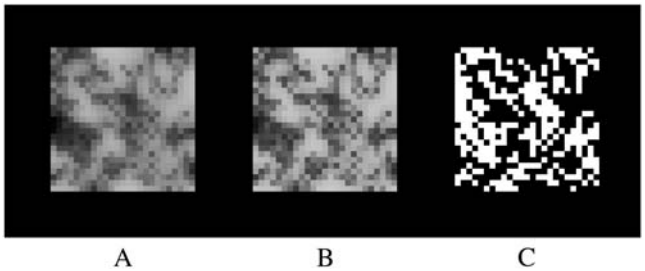

FIGURE 1 A screen-shot of the grid. (*A*) Glucose concentration. (*B*) Lactose concentration. (*C*) The cells on the grid.

A list of all parameters used is given in the Supplementary Material. Quite different parameter values for intracellular dynamics are used in different models of the *lac* operon (8,9,15). We use the parameter values also used in Wong et al. (9). Because the cells can adapt to these parameters, their precise values are less crucial for the outcome. We propose that evolutionary modeling is a good way to deal with the inevitable parameter uncertainty.

We perform three independent simulations for each condition. For each simulation, we trace the last common ancestor. A common ancestor is an individual cell that has all cells at some later time as progeny. Hence the last common ancestor is the last individual cell that has all cells at the end of the simulation as progeny.

To obtain reliable results, while minimizing computational cost, we compete the last common ancestor of each simulation against each other. This is done by initializing a grid with an equal density of two common ancestors. These ancestors are randomly distributed over the grid and the mutation rates are set to zero. If one population dies out, the other population has won the competition. In this way we compete all three last common ancestors pairwise against each other at least 10 times. The simulation yielding the best competitor is chosen to represent that particular condition.

RESULTS

Approximation of the differential equations describing bistability

The equations describing bistability from the previous section can be approximated, such that the cusp bifurcation can be analytically found. Note that only Eqs. 2–6 determine the bistability of the system.

We do not take the cutoff of the transcription rate at $V_{\mathrm{mRNA,\ max}}$ into account. The evolved promoter functions always have maximal transcription rates close to $V_{\mathrm{mRNA,\ max}}$. Furthermore, we will show that bistability with respect to lactose is only determined by the repressed transcription rate.

First we derive an approximation of the equilibrium of Eqs. 2–6. The first three equations are trivial and for the lactose equilibrium we have the equation

$$\overline{P}\left(\frac{k_{\mathrm{Lac,in}} L_{\mathrm{ext}}}{K_{\mathrm{Lac,in}} + L_{\mathrm{ext}}} - \frac{k_{\mathrm{lac,out}} \overline{L}}{K_{\mathrm{Lac,out}} + \overline{L}}\right) = (k_{\mathrm{Lac-Allo}} + k_{\mathrm{cat,Lac}})\overline{B}\,\frac{\overline{L}}{\overline{L} + K_{\mathrm{m,Lac}}} + (\mu + \gamma_{\mathrm{L}})\overline{L}, \quad (12)$$

where $\overline{B}$, $\overline{P}$, and $\overline{L}$ denote equilibrium values. In the bistable region $\overline{L}$ is small compared to the different k-values, and we can neglect the saturated behavior of the model. Furthermore, we use $\overline{B} = \frac{k_B PA(\overline{A},C)}{(\gamma_B+\mu)(\gamma_M+\mu)}$ and $\overline{P} = \frac{k_P PA(\overline{A},C)}{(\gamma_P+\mu)(\gamma_M+\mu)}$ to get

$$\overline{L} = \frac{\xi L_{\mathrm{ext}}}{K_{\mathrm{Lac,in}} + L_{\mathrm{ext}}} \frac{PA(\overline{A},C)}{\zeta PA(\overline{A},C) + 1}, \quad (13)$$

$$\xi \equiv \frac{k_P k_{\mathrm{Lac,in}}}{(\gamma_P + \mu)(\gamma_M + \mu)(\gamma_L + \mu)}, \quad (14)$$

$$\zeta \equiv \frac{\left(\frac{k_P k_{\mathrm{Lac,out}}}{K_{\mathrm{Lac,out}}(\gamma_P + \mu)} + \frac{k_B (k_{\mathrm{cat,Lac}} + k_{\mathrm{Lac-Allo}})}{K_{\mathrm{m,Lac}}(\gamma_B + \mu)}\right)}{(\gamma_L + \mu)(\gamma_M + \mu)}. \quad (15)$$

From Eq. 6 we approximate the allolactose equilibrium up to first-order in $\overline{L}$. To do this, we again assume that $\overline{A}$ is small compared to the different k-values and $(\gamma_A+\mu) \ll \frac{k_{cat,Allo}\overline{B}}{K_{m,Allo}}$. So we assume a linear relationship between the lactose and allolactose concentration and we find

$$\overline{L} = \frac{k_{cat,Allo}K_{m,Lac}}{k_{Lac-Allo}K_{m,Allo}}\overline{A}. \tag{16}$$

$\overline{A}$ can now be found by equating Eqs. 13 and 16:

$$PA(\overline{A}, C) = \frac{\overline{A}}{\frac{\xi L_{ext}}{K_{Lac,in}+L_{ext}}\frac{k_{Lac-Allo}K_{m,Allo}}{k_{cat,Allo}K_{m,Lac}} - \zeta\overline{A}}. \tag{17}$$

This equation gives the equilibrium allolactose concentration for all cAMP concentrations. To study under which conditions bistability occurs, we want to calculate the cusp bifurcation in this model. Writing $x \equiv \overline{A}/k_A$ we get

$$\frac{V_1(1+V_2\mathcal{A}+\frac{V_3}{1+x^m})}{1+V_4\mathcal{A}+\frac{V_5}{1+x^m}} = \frac{x}{\frac{\xi L_{ext}}{K_{Lac,in}+L_{ext}}\frac{k_{Lac-Allo}K_{m,Allo}}{k_{cat,Allo}K_{m,Lac}k_A} - \zeta x},$$

$$\text{where } A \equiv \frac{(C/k_c)^n}{1+(C/k_c)^n} \tag{18}$$

If m were an integer this equation would become a polynomial of power $m+1$, but m is an evolvable parameter, so it has real, noninteger values. Defining $\theta \equiv (\xi L_{ext}/(K_{Lac,in}+L_{ext}))(k_{Lac-Allo}K_{m,Allo})/(k_{cat,Allo}K_{m,Lac}k_A)$ we can rewrite the above to

$$f(x) = ax^{m+1} - bx^m + cx - d = 0, \tag{19}$$

where

$$\begin{aligned} a &\equiv 1 + V_4\mathcal{A} + \zeta V_1(1+V_2\mathcal{A}),\\ b &\equiv \theta V_1(1+V_2\mathcal{A}),\\ c &\equiv 1 + V_4\mathcal{A} + V_5 + \zeta V_1(1+V_2\mathcal{A}+V_3),\\ d &\equiv \theta V_1(1+V_2\mathcal{A}+V_3). \end{aligned} \tag{20}$$

For the cusp bifurcation to take place, $f(x)$, $f'(x)$, and $f''(x)$ need to be zero for the same x-value. So to calculate the condition for the cusp bifurcation we now have to solve the equations

$$\begin{aligned} f(x) &= ax^{m+1} - bx^m + cx - d = 0,\\ f'(x) &= a(m+1)x^m - mbx^{m-1} + c = 0,\\ f''(x) &= a(m+1)mx^{m-1} - bm(m-1)x^{m-2} = 0 \end{aligned} \tag{21}$$

simultaneously. We then find

$$c = b\left(\frac{b(m-1)}{a(m+1)}\right)^{m-1},\ d = a\left(\frac{b(m-1)}{a(m+1)}\right)^{m+1}. \tag{22}$$

From these two equations, the bifurcation parameter L_{ext} can be eliminated by eliminating θ. This is what we want, because we want to know under which parameter conditions a fold bifurcation occurs for a certain value of L_{ext}. After substituting Eq. 20 back, we find, after a long but straightforward calculation, the following condition for the cusp bifurcation, dependent on the cAMP concentration:

$$\lambda(C) \equiv \frac{PA(0,C)}{(m-1)^2}\left(\frac{(m+1)^2}{PA(\infty,C)} + 4m\zeta\right) < 1. \tag{23}$$

If $\lambda(C) < 1$, a fold bifurcation occurs for a certain value of L_{ext}. After the approximations made for the allolactose and lactose equilibrium, this result is exact. We checked this formula for many promoter functions, and the predictions whether the promoter function is bistable are very good. Generally, due to the first-order approximation of the allolactose equilibrium, bistability sometimes also occurs if $\lambda(C)$ is slightly larger than one, but if $\lambda(C)$ is larger than two, bistability never occurs. In the evolutionary simulations, the fluctuations in $\lambda(C)$ are much larger than a factor two, and therefore the approximation is accurate.

From Eq. 15, we observe that ζ determines the ratio of internal lactose that is degraded or transported by operon activity and internal lactose that is degraded, transported, or diluted independently from the operon, $(\gamma_L + \mu)$. The first term of ζ describes lactose efflux by permease and the second lactose degradation via β-galactosidase. Therefore, the only terms that effect bistability are the lactose efflux and degradation terms, and we indeed see that lactose influx, hence inducer exclusion, is not important for bistability.

Artificial inducers are, in contrast to lactose, not degraded by β-galactosidase. This means that ζ is much smaller for artificial inducers than for lactose. The values $k_{cat,\ Lac}$ and $k_{Lac-Allo}$ are zero, and $k_{Lac,\ out}$ and $K_{Lac,\ out}$ will have different values for artificial inducers. These values are reported for the artificial inducer IPTG (16). The value of γ_L is not known, but because there is no degradation of internal inducer by β-galactosidase, there will probably exist a different pathway to degrade the artificial inducer. But even if γ_L is small, we still find that ζ is very small, and Eq. 23 can be approximated by

$$\frac{PA(0,C)}{(m-1)^2}\frac{(m+1)^2}{PA(\infty,C)} < 1. \tag{24}$$

If we now define the repression factor ρ as the ratio of maximal and basal activity, this can be rewritten to

$$\rho(C) \equiv \frac{PA(\infty,C)}{PA(0,C)} > \frac{(m+1)^2}{(m-1)^2}. \tag{25}$$

This limit for artificial inducers is in agreement with a previous study (5), where $\rho > 9$ was derived and a value of $m = 2$ was used. This result is also in agreement with their experiments, which show bistability with artificial inducers for $\rho > 9$, but a continuous response for $\rho \approx 5$. *E. coli* has been reported to have a repression factor >100 (4,5); therefore, bistability is indeed predicted for artificial inducers.

For lactose, the natural inducer, however, the situation is quite different. Because internal lactose is degraded by

β-galactosidase, the fraction between operon-dependent and -independent lactose degradation, ζ, is much larger and the ζ term dominates Eq. 23:

$$\frac{PA(0,C)4m\zeta}{(m-1)^2} < 1. \quad (26)$$

Now we see that, instead of the repression factor ρ, the absolute transcription rate at zero allolactose, $PA(0, C)$, determines whether bistability occurs.

It is not easy to check whether Eq. 26 does or does not hold for the wild-type *lac* operon, because this depends, much more than for artificial inducers, on the detailed parameter values. However, we can compare ζ_{art} and ζ_{lac}, if we use the same value for γ_L, a conservative estimate. We find that $\zeta_{lac} \approx 6000\zeta_{art}$. Therefore, the condition determining bistability for lactose is very difficult to satisfy.

From these findings we conclude that experimental observation of bistability with artificial inducers does not tell much about whether bistability occurs for lactose. Instead of the repression level, the absolute transcription rate at zero allolactose determines whether bistability occurs. But should we expect bistability to occur with lactose as inducer? To study this, we developed the individual-oriented, computational model, explained in the previous section and more detailed in the Supplementary Material, with which we study the in silico evolution of the *lac* operon.

In silico evolution of the *lac* operon

Because we expect, from our results in the previous section, that bistability could be difficult to achieve, we start evolution with a bistable population and study whether bistability remains in the population. We choose values of γ_L and γ_A ($\gamma_L = \gamma_A = 0.15$/min), such that the promoter functions are firmly in the bistable region.

The initial promoter function is plotted in Fig. 2 *A*. Note that initially the induced transcription rate equals $V_{mRNA,\ max}/2$.

Two bifurcation diagrams, corresponding to the promoter function of Fig. 2 *A*, for minimal ($C_{min} \approx 1.0 \times 10^{-5}$ mM) and maximal ($C_{max} \approx 4.8 \times 10^{-4}$ mM) cAMP, i.e., high and low glucose concentration, respectively, are shown in Fig. 2 *B*. These concentrations can be calculated from Eq. 9, using that the minimal and maximal glucose influx are 0 and $k_{t,\ Glu}$, respectively. For all intermediate cAMP concentrations, the bifurcation diagrams lie between these two extremes. The bifurcation diagrams were numerically calculated using the five equations describing bistability (see Methods) and no approximation was used.

The most important parameter determining the outcome of evolution is the cost for *lac* operon activity. We estimate this cost as follows: the fraction of *lac* operon proteins at full activity of the operon is ~3% (17). We assume that the growth rate is also 3% lowered at full activity. We assume a linear relationship between the activity of the operon and the cost. Recently, the cost of the *lac* operon at full activity was measured to be 4–5% (6), which compares well with the value we chose. We performed evolutionary simulations for different environments and cost for *lac* operon activity.

Evolution away from bistability

We can use the bifurcation condition $\lambda(C)$ to follow the switching behavior of all cells in the population. In Fig. 3 *A*, we show the population average of the cusp parameter for minimal and maximal cAMP concentration. Only the population average of $\lambda(C)$ is shown, but the fluctuations in the population are small compared to the fluctuations in the population average and the population is always unimodal. Furthermore note that the fluctuations in $\lambda(C)$ are much larger than the error in the approximation determining $\lambda(C)$. In Fig. 3 *B*, the cAMP concentration at which the cusp bifurcation takes place is shown. This cAMP concentration can be calculated using Eq. 26. If bistability occurs for all cAMP concentrations, we, by default, assign C_{max} (and likewise, C_{min}, if bistability occurs for no cAMP concentration).

We observe that initially evolution drives $\lambda(C)$ rapidly away from the bistable region. This happens for all cAMP concentrations. This behavior is seen in all three independent simulations. In this particular simulation, after only ~3000

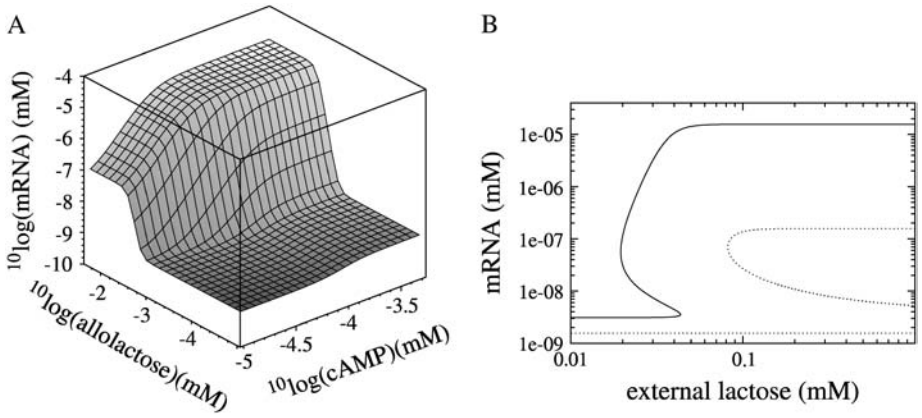

FIGURE 2 (*A*) The initial promoter function of every simulation. (*B*) Two corresponding bifurcation diagrams, for maximal cAMP, i.e., low glucose (*solid line*) and minimal cAMP, i.e., high glucose (*dashed line*). For the bifurcation diagram at high-cAMP, low-glucose concentration, a growth rate of $\mu = 0$/min is used, while for the bifurcation diagram at low-cAMP, high-glucose, a growth rate of $\mu = 0.01$/min is used. Bifurcation diagrams, however, are very similar for different growth rates, because we took $\gamma_L = \gamma_A \gg \mu$.

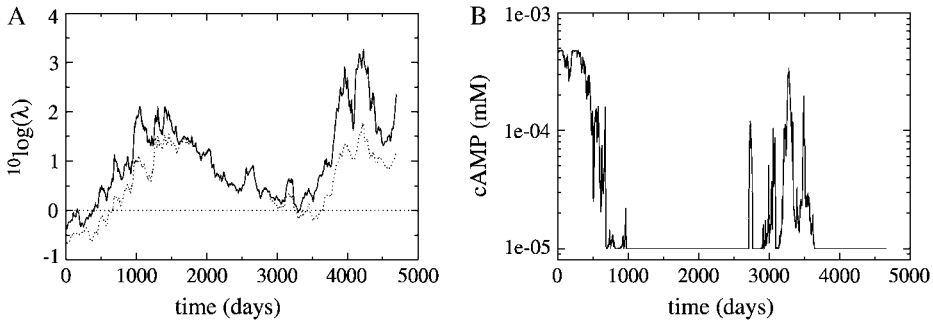

FIGURE 3 (*A*) Population average of the cusp parameter $\lambda(C_{max})$, i.e., low glucose, (*solid line*) and $\lambda(C_{min})$, i.e., high glucose (*dotted line*). (*B*) Population average of the cAMP concentration at which the cusp bifurcation occurs.

days the population is back in the bistable region, but then again rapidly evolves away. Note that the promoter functions that enter the bistable region after ~3000 days are very different from the initial promoter function. The most important difference is the location of the shift, which has gone to a much lower allolactose concentration. This causes the cells almost never to reach the bistable region, because such low external lactose concentrations are very seldom reached.

We can count how many promoter functions are bistable for different cAMP concentrations during all three evolutionary simulations. Not taking into account the initial bistable period, we find that over all three simulations, on average, 9% of the population is potentially bistable for high cAMP, low glucose and 24% for low cAMP, high glucose. In the simulation yielding the best competitor, these percentages are 1.5% and 9%, respectively.

In Fig. 4 we plot the promoter function of the last common ancestor of the evolutionary simulation of Fig. 3, as well as the experimentally observed promoter function (4). Qualitatively, the two promoter functions look strikingly similar. The shifts are very shallow; both in the experiments as in the evolved promoter functions, an ~10-fold increase in inducer concentration is needed to fully induce the operon. Also the four different plateau transcription levels nicely compare with each other. Because in experiments only relative promoter activities are measured, and different experiments yield different quantitative results, a quantitative comparison is not possible.

In Fig. 5 we depict bifurcation diagrams corresponding to the evolved promoter function of Fig. 4 *A*, both for lactose and IPTG as inducer. For lactose, Fig. 5 *A*, no bistability is observed, as was already clear from Fig. 3. For IPTG, however, we see that the promoter function acts bistably for all cAMP concentrations. This is because the repression factor of the evolved operon is indeed high enough (~150) to cause bistability for artificial inducers. Note that we scaled the IPTG concentration with respect to the evolved binding parameter of allolactose to LacI (k_A). IPTG probably has a different binding parameter, but since k_A does not enter the bifurcation condition, the switching behavior is not affected.

Recently the phase diagram of the wild-type lactose utilization network has been measured (5). This phase diagram shows for which external glucose and TMG concentrations the network is bistable, repressed, or induced. Fig. 6 shows this phase diagram for the evolved promoter function of Fig. 4 *A*. The locations of the fold bifurcations were measured in bifurcation diagrams similar to Fig. 5 *B*, for different glucose concentrations. Instead of TMG we again used IPTG as artificial inducer.

Qualitatively as well as quantitatively this phase diagram is very similar to the experimentally observed phase diagram. As in Ozbudak et al. (5), we observe that for high glucose concentrations, the operon becomes induced at higher IPTG concentrations, in a sigmoid way. The reason for this behavior is that when glucose is abundant, there is less need to induce the operon. Quantitatively, the location

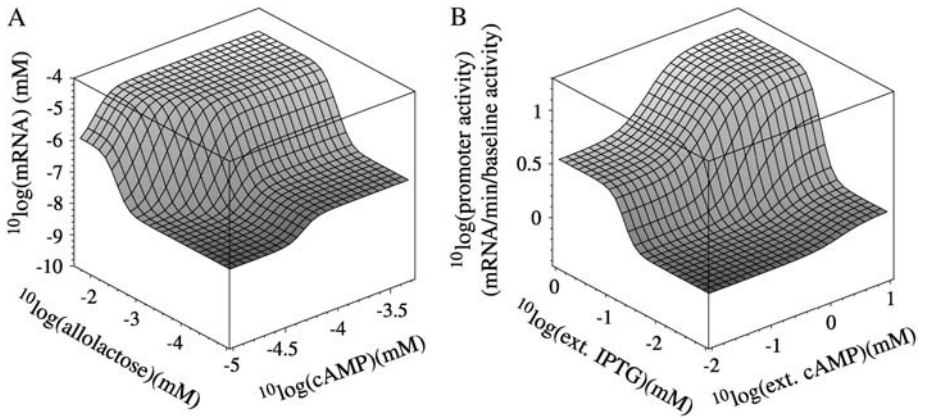

FIGURE 4 (*A*) The promoter function of the last common ancestor with cost of 3%. All evolved promoter functions are only plotted over the cAMP and allolactose concentration the bacterium experiences, which depend on the promoter function itself. (*B*) The experimentally measured promoter function (4).

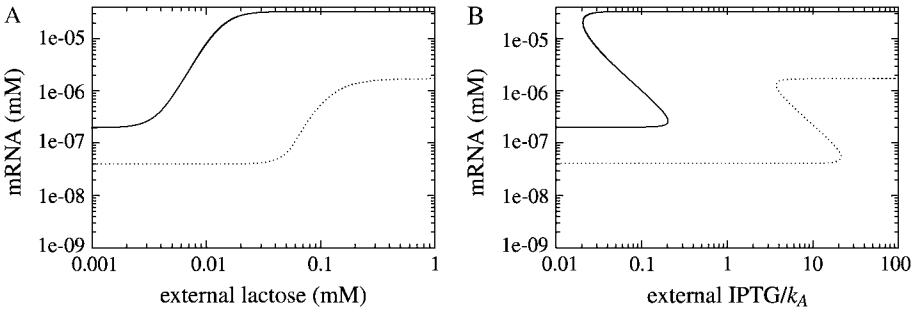

FIGURE 5 Two bifurcation diagrams of the promoter function of Fig. 4 *A*, using lactose (*A*) or IPTG (*B*) as inducer. The solid lines represent maximal cAMP concentration, and the dashed lines minimal cAMP concentration. The same growth rates were used as in Fig. 2.

and the width of the shift from low to high glucose and the width of the bistable region of the evolved promoter function are very similar to that experimentally observed.

Because we did not observe bistability with respect to lactose, we tried to find a condition for which we expect bistability to evolve more easily. If the cost for *lac* operon activity would be higher, it becomes more important to repress activity and bistability might evolve more easily. Therefore we performed evolutionary simulations with unrealistically high cost (10 times higher, such that growth is lowered 30% at full activity).

High cost for promoter activity

The evolutionary dynamics of the cusp parameter $\lambda(C)$ of the simulation is shown in Fig. 7 *A*. Again we see, for high-cAMP, low-glucose concentrations, that the cusp parameter increases and that the population evolves out of the bistable region. For low-cAMP, high-glucose concentrations, however, the opposite is the case. In Fig. 7 *B* the population average of the cAMP concentration at which the cusp takes place is shown.

From Fig. 7 *B* we can see that the cAMP concentration at which the cusp takes place decreases over time. Note that $C_{\min} \approx 1 \times 10^{-5}$ mM. Therefore, only at very high glucose concentrations is bistability maintained. At high glucose concentrations, the bacteria use glucose before using lactose, and when the glucose concentration then decreases, bistability is lost again. In this way, bistability at high glucose could enforce sequential uptake of glucose and lactose.

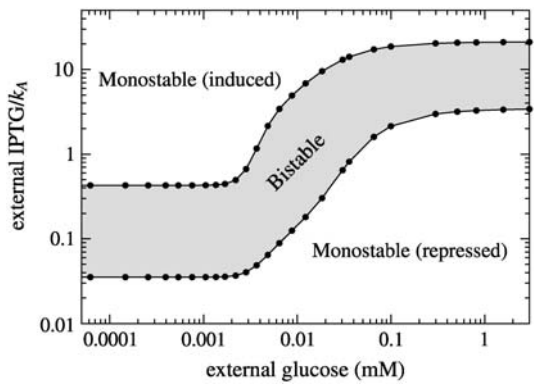

FIGURE 6 Phase diagram corresponding with the promoter function of Fig. 4 *A*. For this picture we used a growth rate of $\mu = 0.01$/min.

However, the cells are too short a time in this part of the phase space to make this bistability functional. For functional bistability, the protein concentrations must be able to adapt to the transcription rate, which, due to the low protein degradation rate, takes hours. In the mean time, glucose is rapidly consumed by the cells and the glucose concentration drops below the glucose concentration required for bistability before the protein concentrations reach their equilibrium values. In Fig. 7 *C* we show how often cells are on a certain position in the phase space. We can see that the low-allolactose, low-cAMP corner is indeed rarely visited by the cells. Still, the low promoter activity in this region lowers cost and enlarges the delay in lactose uptake in the presence of glucose.

The promoter function of the last common ancestor of this simulation is shown in Fig. 7 *D*, and the corresponding bifurcation diagram for lactose and IPTG, respectively, in Fig. 7, *E* and *F*. For artificial inducers, the evolved promoter function again behaves bistably for all glucose concentrations, whereas this only happens at very high cAMP levels when induced by lactose.

For high cost, on average 24% of the population is bistable for low glucose and 73% for high glucose. These averages are again calculated over all three evolutionary simulations. Indeed, for high cost, bistability is more likely, but is still most often avoided for low glucose concentrations.

Another important difference between the two costs is the location of the shift between low and high allolactose concentrations that evolves. For high cost, the operon becomes induced at approximately a 10-times higher allolactose (and hence external lactose) concentration (compare Fig. 4 *A* and Fig. 7 *D*). This is because when the cost for promoter activity is high, it does not pay to be active at relative low external lactose concentrations, whereas it does when the cost is lower.

Longer and shorter periods with and without lactose influx

In different environments, different promoter functions might evolve. Therefore, we checked our results for different

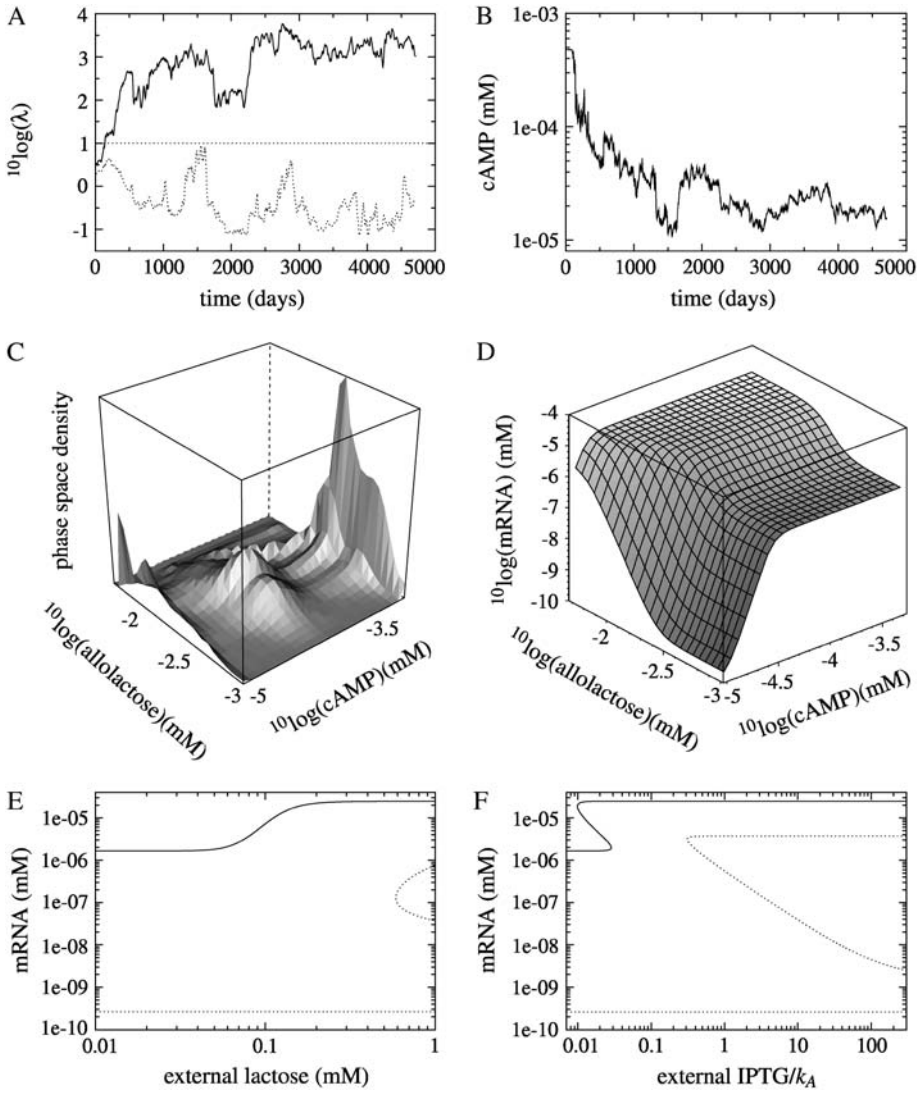

FIGURE 7 Results of evolution with high cost for promoter activity. (*A*) Population average of the cusp parameter $\lambda(C_{max})$ (*solid line*) and $\lambda(C_{min})$ (*dotted line*). (*B*) Population average of the cAMP concentration at which the cusp bifurcation occurs. (*C*) Histogram of the number of visits of the promoter function shown in Fig. 7 *D* in cAMP-allolactose space. (*D*) The promoter function of the last common ancestor. (*E*) The bifurcation diagram, corresponding to the promoter function in Fig. 7 *D*, when growing on lactose, for maximal-cAMP, low-glucose (*solid line*) and minimal-cAMP, high-glucose (*dashed line*). Again the same growth rates were used as in Fig. 2. (*F*) Bifurcation diagrams using IPTG as inducer.

durations of periods with and without influx. Increasing the duration (with a factor two) of periods without lactose influx might increase the cost for having a high repressed transcription rate and therefore favor bistability. However, we again found similar results.

Decreasing the duration of the periods, both with and without glucose and lactose (by a factor four), leads to a decrease in regulation. Because there is too little time between periods of lactose influx, the cells choose to stay active at low lactose concentrations. This is seen in three independent simulations.

In one simulation, the population totally lost regulation with respect to lactose at low glucose concentrations. However, the last common ancestor of this simulation was the least competitive. The two other last common ancestors were competitively equal. One of these ancestors is shown in Fig. 8. At low-glucose, low-lactose, this ancestor decreases its activity only by approximately factor-two. At very high glucose concentrations however, it exhibits bistability, in the same way as the high cost promoter function.

The third promoter function has a very shallow slope relative to lactose: Only at low lactose concentrations appreciable regulation occurs. At very low lactose concentrations the promoter function is bistable, for all glucose concentrations. Such low lactose concentrations are, however, very seldom encountered, due to the frequent switching of the environment, and again the bistability is not functional. If the occurrence of these very low lactose concentrations is enforced by removal of external lactose, the promoter functions evolved away from bistability, again in three independent simulations.

Why to avoid bistability?

In Fig. 9 we plot the shifting behavior, from a lactose-poor to a lactose-rich environment, of seven different promoter

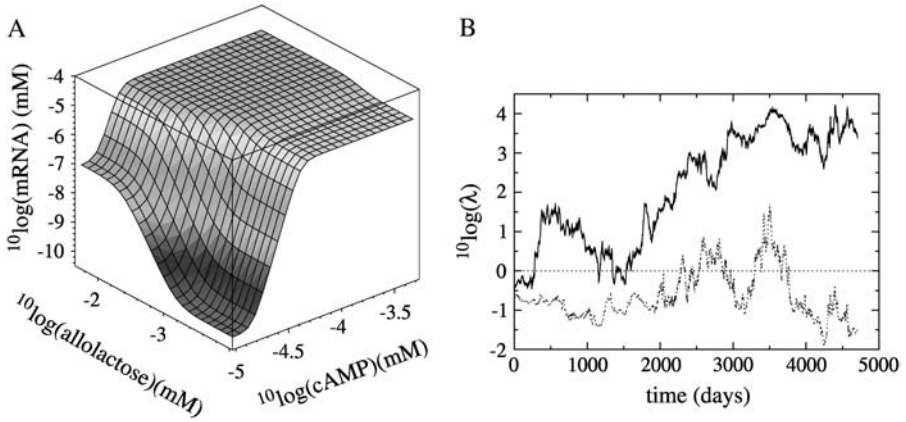

FIGURE 8 (*A*) The promoter function of one of the two most competitive last common ancestors. (*B*) Population average of the cusp parameter $\lambda(C_{\max})$ (*solid line*) and $\lambda(C_{\min})$ (*dashed line*).

functions, differing in only one parameter (γ, see Supplementary Material). This parameter, which gives the leakiness of the promoter function, changes the transcription rate at zero allolactose, ($PA(0, C)$). The external lactose, mRNA, and permease concentration are shown.

When influx starts after 10 min, we see that the highest four promoters immediately become induced, whereas for the lowest three it takes a while before they become induced. The lower three promoter functions are bistable, and the external lactose concentration has to increase over a certain threshold before they become induced. But we also see for continuous switches that the higher $PA(0, C)$, the faster the switch.

The doubling-time of *E. coli* is ~1 h, of the same order of the delay in lactose uptake. For wild-type *E. coli* it also takes ~1 h after induction, before the protein concentrations are maximal. Therefore, decreasing its delay can give a cell a very significant growth advantage. This explains why the population evolves out of the bistable region.

Thattai and Van Oudenaarden (18) explain advantageousness of bistability using a model with instantaneous switching between equilibria. We now see that the crucial factor determining the (dis)advantageousness of bistability is the fact that switching between the two equilibria is not instantaneous, because of the slow protein dynamics. Because the difference between induced and repressed transcription levels is higher for bistable promoters, switching is slower for bistable promoters than for continuous promoters.

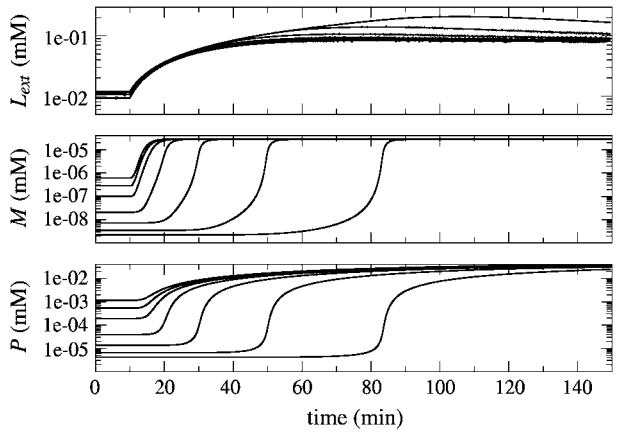

FIGURE 9 Dynamics of L_{ext}, M, and P during a shift from a lactose-poor to a lactose-rich environment. The different lines correspond to different promoter functions, which are only different in one parameter, which determines $PA(0, C)$.

DISCUSSION

The response of the *lac* operon to artificial inducers has had much attention, but from an evolutionary point of view, only the behavior with respect to lactose is important. Lacking information about the behavior of the operon with respect to lactose, the results for artificial inducers have been extrapolated to lactose.

However, only recently the response of the *lac* operon to lactose has been investigated (4,5) and no bistability has been demonstrated (5). From our results, this is only to be expected. The analytical expression we derived, simultaneously describes the switching behavior of the operon with respect to artificial inducers and to lactose. For artificial inducers we indeed find that the promoter function is in the bistable region. Due to the fact that lactose is metabolized by β-galactosidase, it is much less likely that the operon is bistable with respect to lactose. Direct observation whether the *lac* operon is bistable with respect to lactose is still difficult (5). Our analytical result can predict whether or not the operon is bistable with respect to lactose. For this prediction we would need to know how large the operon-independent lactose decay and transport is, and a reliable estimate for the protein concentrations for the repressed operon.

It has already been claimed that bistability with respect to lactose would not be possible (19). In that model, however, no operon-independent degradation is taken into account. In our model, this is described by the limit $\lim_{\zeta \to \infty} \lambda(C) = \infty$, and therefore, in that limit, bistability can indeed never be found. We find, like Yildirim and Mackey (8), however, that due to growth or possible mechanisms to degrade internal

lactose (γ_L), bistability for lactose is also possible, albeit much more difficult than for artificial inducers.

The evolved promoter function for realistic operon cost strikingly resembles the experimentally observed promoter function (4), especially in the simulation yielding the best competitor. High transcription rates at zero allolactose and shallow shifts were experimentally observed, and this is also what we find. Both these properties help to avoid bistability when growing on lactose, which is a strong indication that the operon indeed evolved to avoid bistability. Furthermore, the phase diagram of the *lac* operon, when growing on an artificial inducer, is almost identical to the experimentally observed phase diagram (5).

In different environments or with different parameters, different promoter functions evolve. Interestingly, which promoter function evolves again shapes the environment the cells experience. At high cost, for example, the promoter function evolves such that cells never experience lactose concentrations as low as those evolved at low cost, because the cells evolved at high cost do not deplete lactose to such low levels.

Because cells never experience extremely low lactose levels, bistability at very low lactose concentrations is nonfunctional. We performed simulations in which we enforced very low lactose concentrations by adding an external decay for glucose and lactose, such that bistability is more often functional. Indeed, a population with nonfunctional bistability at these low lactose levels evolves out of the bistable region when lactose decays externally.

We have opted to study evolution of the *lac* operon in a spatially explicit model, because previous work (14,20) has shown that a spatial context favors the evolution of regulation, in contrast to evolutionary adaptation (compare (6)). In particular, space appears to be crucial when regulatory states last over many generations (20), as is the case for the *lac* operon.

Furthermore, a spatial model ensures that the environment of the cells changes over multiple timescales. The glucose and lactose influx period define a long timescale. Due to cell division and movement, cells also experience changes in the environment over a much shorter timescale. In this way, space makes the environment of the cells inherently noisy. Without space, cells ''know'' that if the lactose concentration starts increasing, it will keep increasing for a long time. Bistability can in theory function as a noise-filter of a system, which makes space an important factor to consider.

The search space in the evolutionary simulations is very high-dimensional and redundant. We found that minimizing the dimensionality of the search space, as is done in the mathematical analysis, by evolving the V parameters instead of the biological parameters, decreases the search efficiency. This is in agreement with the known role of neutrality in evolution (21).

Our evolutionary simulations clearly point out that bistability is disadvantageous for the cells, due to the increase in delay in lactose uptake it causes, especially in the absence of glucose. Even with unrealistically high cost, bistability is only observed for very high glucose concentrations. This bistability is nonfunctional as we explained above.

We used a deterministic model to describe the intracellular dynamics of each cell. It is known, however (22), that protein numbers in the repressed *lac* operon are low. Therefore, stochasticity might play an important role in regulation of the *lac* operon.

A bistable cell can, due to stochasticity, switch between both equilibria. In this way the population can become heterogeneous, a phenomenon called bet-hedging, which could be beneficial, because a fraction of the population will always be in the best state.

Recently, there has been a lot of interest in the circumstances under which bet-hedging would be beneficial. It has been shown that bet-hedging strategies can be beneficial when environmental sensors are imperfect or when the cost for sensing the environment is high enough (23,24). Without any sensor imperfection or cost, bet-hedging can still be beneficial in periodic environments, but not in a stochastic environment (18).

However, all these studies assume instantaneous switching between intracellular states. We now show that the crucial factor determining the disadvantage of bistability is the increase in delay in switching between the equilibria. Because the repressed transcription rate must be very low for bistability to occur, it takes much time to switch between both equilibria, even when stochasticity allows switching in the bistable region. These crucial considerations are neglected in these previous models.

Our study indicates that a priori we should expect the *lac* operon not to be bistable, because of the mentioned disadvantages. Whether bet-hedging due to stochasticity can overcome these disadvantages remains to be seen. Preliminary simulations, in which stochasticity is incorporated, suggest that bistability is avoided in the same way as described in this article. As stochasticity is a very important issue in this context, we will further investigate the effects of stochasticity in our model.

In any case, our results suggest that no advantages for bistability need to be sought. From our mathematical analysis it is clear that bistability is much more difficult for lactose than for artificial inducers, and that the wild-type promoter probably is not bistable with respect to lactose. Furthermore, our evolutionary results show that bistability is disadvantageous and therefore avoided during evolution. Finally, experimentally, bistability has not been observed for lactose, although it has been for artificial inducers (5).

In evaluating the promoter function, we should be aware that there is no such thing as ''the'' promoter function of *E. coli*. It has been shown that a population of *E. coli* cells can adapt to new environments by changing the operon activity in only a few hundred generations (6), and that prolonged absence of lactose can even destroy regulation altogether. In

our model, prolonged absence of lactose can push the promoter function into the bistable region. Our results suggest that these so-evolved individuals will lose out when lactose becomes an essential metabolite once again. All in all, we conclude that there is now ample evidence that bistability in the *lac* operon of *E. coli* is an artifact of using artificial inducers and it has not evolved for lactose.

SUPPLEMENTARY MATERIAL

An online supplement to this article can be found by visiting BJ Online at http://www.biophysj.org.

We thank Athanasius Marée for helpful discussion.

REFERENCES

1. Jacob, F., D. Perrin, C. Sanchez, and J. Monod. 1960. Operon: a group of genes with the expression coordinated by an operator. *C. R. Hebd. Seances Acad. Sci.* 250:1727–1729.
2. Griffith, J. S. 1968. Mathematics of cellular control processes. II. Positive feedback to one gene. *J. Theor. Biol.* 20:209–216.
3. Novick, A., and M. Weiner. 1957. Enzyme induction as an all-or-none phenomenon. *Proc. Natl. Acad. Sci. USA.* 43:553–566.
4. Setty, Y., A. E. Mayo, M. G. Surette, and U. Alon. 2003. Detailed map of a *cis*-regulatory input function. *Proc. Natl. Acad. Sci. USA.* 100:7702–7707.
5. Ozbudak, E. M., M. Thattai, H. N. Lim, B. I. Shraiman, and A. Van Oudenaarden. 2004. Multistability in the lactose utilization network of *Escherichia coli*. *Nature*. 427:737–740.
6. Dekel, E., and U. Alon. 2005. Optimality and evolutionary tuning of the expression level of a protein. *Nature*. 436:588–592.
7. Chung, J. D., and G. Stephanopoulos. 1996. On physiological multiplicity and population heterogeneity of biological systems. *Chem. Eng. Sci.* 51:1509–1521.
8. Yildirim, N., and M. C. Mackey. 2003. Feedback regulation in the lactose operon: a mathematical modeling study and comparison with experimental data. *Biophys. J.* 84:2841–2851.
9. Wong, P., S. Gladney, and J. D. Keasling. 1997. Mathematical model of the lac operon: inducer exclusion, catabolite repression, and diauxic growth on glucose and lactose. *Biotechnol. Prog.* 13:132–143.
10. Postma, P. W., J. W. Lengeler, and G. R. Jacobson. 1993. Phosphoenolpyruvate:carbohydrate phosphotransferase systems of bacteria. *Microbiol. Rev.* 57:543–594.
11. Malan, T. P., A. Kolb, H. Buc, and W. R. McClure. 1984. Mechanism of CRP-cAMP activation of lac operon transcription initiation activation of the P1 promoter. *J. Mol. Biol.* 180:881–909.
12. Hogema, B. M., J. C. Arents, R. Bader, and P. W. Postma. 1999. Autoregulation of lactose uptake through the LacY permease by enzyme IIAGlc of the PTS in *Escherichia coli* K-12. *Mol. Microbiol.* 31:1825–1833.
13. Andersen, K. B., and K. Von Meyenburg. 1980. Are growth rates of *Escherichia coli* in batch cultures limited by respiration? *J. Bacteriol.* 144:114–123.
14. Pfeiffer, T., S. Schuster, and S. Bonhoeffer. 2001. Cooperation and competition in the evolution of ATP-producing pathways. *Science.* 292:504–507.
15. Santillan, M., and M. C. Mackey. 2004. Influence of catabolite repression and inducer exclusion on the bistable behavior of the lac operon. *Biophys. J.* 86:1282–1292.
16. Cheng, B., R. L. Fournier, P. A. Relue, and J. Schisler. 2001. An experimental and theoretical study of the inhibition of *Escherichia coli* lac operon gene expression by antigene oligonucleotides. *Biotechnol. Bioeng.* 74:220–229.
17. Koch, A. L. 1983. The protein burden of lac operon products. *J. Mol. Evol.* 19:455–462.
18. Thattai, M., and A. Van Oudenaarden. 2004. Stochastic gene expression in fluctuating environments. *Genetics.* 167:523–530.
19. Savageau, M. A. 2001. Design principles for elementary gene circuits: elements, methods, and examples. *Chaos.* 11:142–159.
20. Pagie, L., and P. Hogeweg. 2000. Information integration and red queen dynamics in coevolutionary optimization. *In* Proceedings of the 2000 Congress on Evolutionary Computation CEC00. IEEE Press, La Jolla Marriott Hotel, La Jolla, California.1260–1267.
21. Huynen, M. A., P. F. Stadler, and W. Fontana. 1996. Smoothness within ruggedness: the role of neutrality in adaptation. *Proc. Natl. Acad. Sci. USA.* 93:397–401.
22. Kierzek, A. M., J. Zaim, and P. Zielenkiewicz. 2001. The effect of transcription and translation initiation frequencies on the stochastic fluctuations in prokaryotic gene expression. *J. Biol. Chem.* 276:8165–8172.
23. Wolf, D. M., V. V. Vazirani, and A. P. Arkin. 2005. Diversity in times of adversity: probabilistic strategies in microbial survival games. *J. Theor. Biol.* 234:227–253.
24. Kussell, E., and S. Leibler. 2005. Phenotypic diversity, population growth, and information in fluctuating environments. *Science.* 309: 2075–2078.